2020

Joint Shelf Design and Shelf Space Allocation Problem for Retailers

Hakan Gecili
Wright State University

JOINT SHELF DESIGN AND SHELF SPACE ALLOCATION PROBLEM FOR RETAILERS

A dissertation submitted in partial fulfillment of the
requirements for the degree of
Doctor of Philosophy

By

HAKAN GECILI
B.S., Turkish Naval Academy, Turkey, 2002
M.S., Kocaeli University, Turkey, 2012

2020

Wright State University

WRIGHT STATE UNIVERSITY

GRADUATE SCHOOL

Jun 24, 2020

I HEREBY RECOMMEND THAT THE DISSERTATION PREPARED UNDER MY SUPERVISION BY Hakan Gecili ENTITLED Joint Shelf Design and Shelf Space Allocation Problem for Retailers BE ACCEPTED IN PARTIAL FULFILLMENT OF THE REQUIREMENTS FOR THE DEGREE OF Doctor of Philosophy.

Pratik Parikh, Ph.D.
Dissertation Director

Brian Rigling, Ph.D
Interim Director, Engineering PhD Program, Professor and Dean, College of Engineering and Computer Science

Barry Milligan, Ph.D.
Interim Dean of the Graduate School

Committee on Final Examination:

Pratik Parikh, Ph.D.

Xinhui Zhang, Ph.D.

Subhashini Ganapathy, Ph.D.

Nan Kong, Ph.D.

Amir Zadeh, Ph.D.

ABSTRACT

Gecili, Hakan Ph.D., Engineering Ph.D. program, Wright State University, 2020. Joint Shelf Design and Shelf Space Allocation Problem.

Although the retail business has been exploring innovative ways to engage shoppers, the COVID-19 pandemic has sped up their effort. Because of its unique benefits, physical stores will continue to remain an integral part of the overall retail business. However, to stay competitive, retailers will be forced to effectively utilize their available space in physical store (and even reduce it if need be), while offering a reasonably large assortment of products on their shelves. For many such retailers, the design of planograms – visual representation of products on shelves – is still driven by prior experience and intuition. Further, existing optimization-based planogram design approaches assume that the shelf length and height are fixed, which often result in unused space on the planogram or suboptimal assignment of SKU facings, both resulting in reduced revenue for the retailer.

To address this real-world challenge, we introduce the joint shelf design and shelf space allocation (JSD-SSA) problem to maximize retailer's revenue. Our proposed mathematical programming model for JSD-SSA determines the optimal shelf design, while determining SKU placement and facings, under SKU family constraints. Because realistic problem sizes pose significant computational challenges in solving this model, we propose a decomposition-based approach. Accordingly, we first partition the planogram area and allocate it to each SKU family via a Particle Swarm Optimization heuristic, then for each partition we determine the shelf design (number of shelves, shelf coordinates, length, and height) and shelf space allocation (SKU

placement and facings) using Constraint Programming. In so doing, real-world problem instances (2 families, 100 SKUs total, 192” × 84” planogram size) could be solved within 45 minutes. We also propose a metric to measure variation in SKU shapes within and between SKU families.

Our experiments indicate that shorter shelf lengths can increase retailer’s profit by up to 22% depending on the SKU-family shape variation. Higher within-family shape variation can result in higher revenue increases. Further, as the planogram becomes tighter (measured via space tightness), the benefits of shorter shelf lengths increase. Additionally, if SKU and planogram dimensions share a common factor or multiple, then more compact planograms can be designed, in turn reducing unused space and increasing retailer’s profit.

We strongly believe that our optimization-based approach will allow retailers to fully utilize the available shelf space, especially during post COVID-19 environment where retailers may opt to reduce their store footprint. Better SKU allocation on highly visible shelf locations will allow better shopper-SKU interaction, in turn reduce expensive trial-and-errors. Our approach will also allow benchmarking of existing and alternative planogram designs depending on the location of the department in the store and corresponding shopper traffic.

TABLE OF CONTENTS

LIST OF FIGURES

LIST OF TABLES

ACKNOWLEDGEMENTS

I would like to offer my special thanks to Dr. Pratik Parikh for his continuous support and guidance during the development and delivery of this research. Dedication of his time and personal support has been greatly appreciated.

Thank you Dr. Xinhui Zhang for your constant help and supervision for many years, which changed my life and facilitated this research. I also appreciate the valuable suggestions and comments of my committee.

To Melanie Gecili, thank you for your support and friendship through the transition of my life and education.

To my son Deniz Kaan Gecili and my parents Veli and Kevser Gecili, thank you for all the love and support.

Finally, I want to thank all my friends and family for encouraging me to pursue my degree.

1. INTRODUCTION

The proliferation of new products and product variants, changes in customers' expectations, finite and scarce retail shelf space, and thin profit margins make the retail industry very competitive (Curhan, 1972; Zufryden, 1986; Lim et al., 2004; J. M. Hansen et al., 2010). To meet the dynamic demand under limited space, retail managers frequently attune their assortments and planograms (J Irion et al., 2011); improved space utilization via effective space management approaches have become even more critical to stay competitive (Geismar et al., 2015).

A common problem in this area is the Shelf Space Allocation (SSA); i.e., the decision of which products are selected and how many faces are shown. The goal of SSA is to increase sales of a product by increasing its perceptibility (P. Hansen & Heinsbroek, 1979), reduce stock-outs, and decrease managerial expenses such as labor cost (Lim et al., 2004) by accounting for computer-aided shelf space management approaches to enhance customer satisfaction have, therefore, become popular (Yang, 2001).

Although a variety of approaches have been presented to address the SSA, some of which account for demand characteristic (substitution, space, and cross-space elasticity), varying features of products (types, dimensions, prices, families), and other merchandising constraints, they all either ignore shelves or assume that the shelf dimensions are prespecified. Researchers, ignoring the shelf structure, use only one dimension of products (area, space or length) and assume that products have a liquid form. However, most product packagings are reasonably rigid and have specific geometry. Studies that acknowledge that products have a unique shape (slot allocation) or they can fit on shelves no matter what the allocation is, assume a fixed shelf design. However, a mismatch between product geometry and the shelf opening can create unused space between the top of products and the shelves above them. While shelf space allocation is also jointly considered with assortment planning in many studies (Borin et al., 1994; Smith & Agrawal, 2000; Kök & Fisher, 2007; J Irion et al., 2011; Jens Irion et al., 2012), the deficiencies mentioned here are even more pronounced in those setups. Because new product dimensions in an adjusted assortment can make the layout infeasible, therefore a new assortment can dictate a new shelf design.

Interestingly, our observations at stores of nearby retailers suggest that stores commonly use different sized bays for gondola and peg shelves. These types of racks can accommodate shelves with different height and lengths. As for 2020, most commonly used shelf lengths are 24 in., 36 in., 48 in. and heights are 54 in., 60 in., 72 in. and 84 in. Besides, products come with many shapes and sizes, and retailers use mixed shelf lengths and heights in an attempt to efficiently utilize the planogram area (Figure 1).

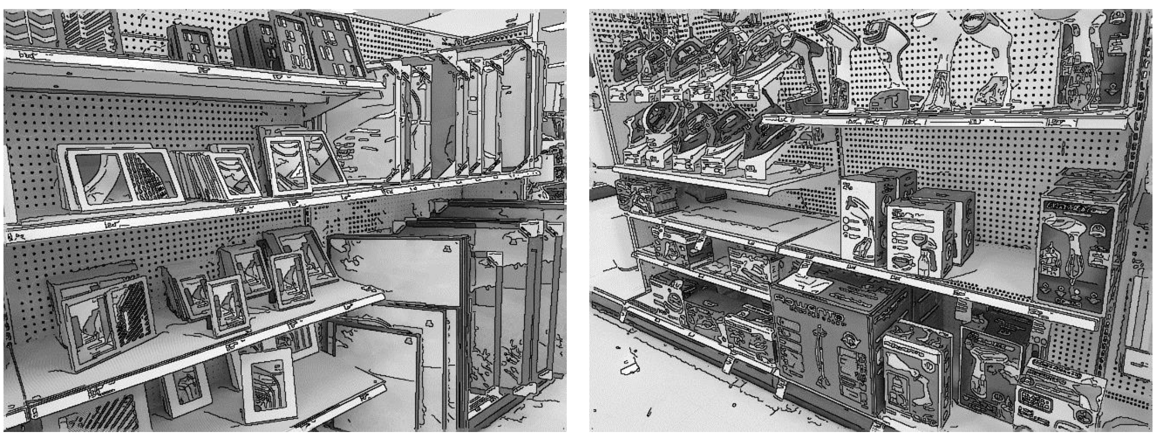

Figure 1. Gondola shelves with mixed length and height

The lack of scientific approaches to determine the best configuration of their shelves and allocate products to it, in turn, results in retailers resorting to expensive trial-and-errors. This begs the question: *What would the ideal mix of shelf lengths and heights on a rack that achieves this goal? How much more would the expected revenue increases be? Would such configurations be optimal in all settings? What factors affect the design of such shelves?*

To the best of our knowledge, the joint problem of shelf design and shelf space allocation has yet to be studied. In this paper, we propose an optimization-based approach for, what we now refer to as, the Joint Shelf Design and Shelf Space Allocation (JSD-SSA) problem. In so doing, we make the following contributions:

1. We propose a Mixed Integer Programming (MIP) model for JSD-SSA, which determines the number of shelves, their height, length, and position on a 2D planogram, along with the standard SSA decisions by taking the adjacency and alignment constraints of product families into consideration. The objective of JSD-SSA is to maximize retailers' daily revenue per planogram.
2. While small instances of this problem can be solved efficiently using a commercial solver, realistic problem sizes (e.g., 100 products, planogram height 72" and length 120") pose significant computational challenges. Our proposed hybrid approach decomposes the problem into two subproblems: (i) SKU family-to-location and (ii) shelf-sizing and product placement. This approach effectively uses the Particle Swarm Optimization (PSO) to solve subproblem (i) and, for each particle, uses Constraint Programming (CP) to solve subproblem (ii). We compare the performance of our proposed approach to CPLEX and CP-only approaches on small instances to demonstrate its viability.
3. We evaluate the sensitivity of the derived solutions to varying levels of heterogeneity in SKU sizes and planogram sizes. Our experiments are based on real data, which is derived from more than 35,000 planograms available from a leading US retailer. In so doing, we generate managerial insights of immediate use for the retailers.

Based on our experiment designs, we observe that as the homogeneity increases, the model tends to create longer shelves, and as the heterogeneity increases the model creates mixed shelf length and heights. Our experiment results showed that as planogram space gets tighter, shorter shelves become more beneficial. We also observed that if SKU shapes are heterogeneous, the proposed shelf design model can increase the profit by 22%. Finally, we found that the allocation of SKUs sharing a common factor or multiples in SKU dimensions, and the planogram dimensions tend to utilize the planogram space better.

The rest of the article is structured as follows: Section 2 outlines the literature review of Shelf Space Allocation. Section 3 builds the mathematical model for shelf design and SKU allocation, and Section 4 describes the decomposition-based solution approach. Section 5 describes the retail data, experimental study, and presents key insights for retailers. Section 6 represents a case study. Finally, we summarize the key findings and propose future studies in Section 7.

2. LITERATURE REVIEW

Shelf space allocation problem has been studied at three levels; store-wide, category-level, and shelf-level (A. H. Hübner & Kuhn, 2012). Store and category planning studies consider exposure to customer traffic as visibility and use the customer traffic distribution to optimize their design (Chen & Lin, 2007; Flamand et al., 2016, 2018; Guthrie & Parikh, 2020).

Considering the focus of our work, below we now summarize the literature in the areas of shelf-level space planning, that focus on determining the number of faces and locations of each SKU.

2.1. Shelf space allocation

Shelf space allocation studies date back to the 1970s and are often modeled as Bounded Knapsack Problem (BKP) or Multi Knapsack Problem (MKP). A Knapsack Problem (KP) is called BKP, if the decision-maker determines the number of items to carry and it is called MKP if there is more than one knapsack (Martello & Toth, 1990). From the KP point of view, SSA models are considered as BKP, where retailer decides the number of faces of each SKU. Some SSA models divide the planogram area into multiple shelves (with prespecified dimensions) and solve the SSA problem as an MKP (Yang, 2001).

In most SSA models demand is modeled by using elasticity (space/price) and inventory terms. In the retail industry, space elasticity is defined as an increase/decrease in demand in response to changes in the space of a product. Shelf space elasticity has been considered in several SSA studies (Brown & Tucker, 1961; Corstjens & Doyle, 1981; J. M. Hansen et al., 2010; Jens Irion et al., 2012; A. Hübner & Schaal, 2017; Bianchi-Aguiar et al., 2018) and assortment planning models (P. Hansen & Heinsbroek, 1979). However, some later studies preferred simplicity and linearized their models by excluded the elasticity terms (Yang & Chen, 1999; Yang, 2001).

Many SSA studies further include inventory decisions into their models, as SSA is closely associated with inventory. Various aspects of inventory were incorporated into SSA. Corstjens & Doyle (1983) studied the inventory of products with increasing demand trends, Bai & Kendall (2008) modeled the effect of the freshness of inventory in SSA, Urban (2002) and Hariga et al. (2007) examined the impact of declining shelf inventory on SSA. More complicated models incorporated inventory decisions with SSA and assortment planning (Urban, 1998, 2002). For a detailed literature review on SSA, we refer to Hübner & Schaal (2017). However, these prior works do not consider the positions of SKUs. Consequently, shelf design is not a part of their models

2.2. Planogram layout

Planogram layout optimization models calculate the number of faces considering positioning and merchandising rules. Positioning rules typically include non-overlapping SKU allocation, shelf dimensions, stocking and orientation of SKUs, and horizontal/vertical location effects.

Merchandising rules dictate some clustering and replenishment constraints on layout optimization. Customers expect to see similar products together; brands can buy positions on shelves to compete better. Available labor can dictate the number of faces on shelves due to limited replenishment frequency and amount. Hwang et al. (2009) considered the rectangular area and adjacency constraints by partitioning the planogram area for SKUs using guillotine cuts. They created a model similar to facility design models and solved it through a genetic algorithm. Russell & Urban (2010) presented a mixed-integer quadratic layout optimization model, which takes the product adjacency and vertical and horizontal location effects into consideration. Geismar et al. (2015) allocated products in a rectangular area in their unit length shelf-space allocation model for a DVD store. Bianchi-Aguiar et al. (2018) proposed a mixed-integer model to allocate families of SKUs in rectangular clusters by considering their family hierarchy. A recent study by A. Hübner et al. (2020) partitioned the shelf area into rectangles and assigned facings in 3D (X-Y-Z). They solved the layout and assortment planning problem jointly by using a genetic algorithm.

Horizontal/vertical location effects on demand have been discussed by many authors, with some conflicting evidence. Models considering these effects assume that SKUs at eye level are more visible and have higher impulse purchase rates. Frank &Massy (1970) used multiple regression analysis to estimate location effects and concluded that height does not have a significant impact on sales. However, Drèze et al. (1994) suggested that horizontal location does not have a notable effect on sales, however, the vertical location does. The horizontal location effect was also examined by van Nierop et al. (2008) where they evaluated the interaction between the shelf layout and marketing activities. They concluded that horizontal location/promotion effects are weak for products that are not close to a racetrack. Yet, J. M. Hansen et al. (2010) argued that the number of facings and vertical/horizontal positions have a significant effect on items' profitability.

Some other positioning considerations in layout optimization are stackable and rotatable products and inventory. Stacking and orientation variables enable better utilization of the shelf area, and they were studied by Murray et al. (2010) and Bai et al. (2013). The layout and inventory were studied jointly by Hwang et al. (2005), in which they proposed a model to determine how much of an item to order, how many facings to allocate, and where to allocate them. They solved their model using a gradient search heuristic and a genetic algorithm.

Table 1. Shelf space allocation models

Model	Authors
No positioning	P. Hansen & Heinsbroek, 1979; Corstjens & Doyle, 1981, 1983; Zufryden, 1986; Bultez & Naert, 1988; Borin et al., 1994; Urban, 1998, 2002; Yang & Chen, 1999; Yang, 2001; Lim et al., 2004; Bai & Kendall, 2005, 2008; Hariga et al., 2007; Gajjar & Adil, 2011; A. Hübner & Schaal, 2017
Fixed shelf length and height	van Nierop et al., 2008; J. M. Hansen et al., 2010; Murray et al., 2010; Russell & Urban, 2010; Bai et al., 2013; Geismar et al., 2015; Bianchi-Aguiar et al., 2018
Planogram area partitioning	Hwang et al., 2009; A. Hübner et al., 2020

Our review of the extant literature indicates that previous studies either ignore the existence of shelf structure or they assume that shelves are fixed or given (Table 1). However, retail shelf bays have slots (see Figure 1) to enable retailers to adopt varying shelf positions according to product types. We do not know of any model in the academic literature that would allow retailers to jointly optimize the shelf design and SSA decisions to maximize their revenue. Through this research, we address this gap in the SSA literature and detail our approach below.

3. A MODEL FOR THE JSD-SSA PROBLEM

The JSD-SSA in this paper is defined as follows; given a planogram space and assortment which shelf design and SKU allocation can yield the maximum profit? Shelf design is controlled by the number of shelves, their dimensions (length, height), and coordinates (vertical, horizontal). SKU allocation is done by determining the number of faces and their coordinates in a 2D plane.

We make the following assumptions in developing our model:

- The assortment and dimensions of SKUs, and the planogram area are known; upper bounds and family clusters for each SKU are given.
- All SKUs must be allocated; product orientation and stacking decisions are known a priori.
- The visual location effect in both horizontal and vertical directions is uniform.
- Products are assumed to have a rectangular shape; if the product shape is not rectangular, then the minimum-encapsulating rectangle (bounding-box) is assumed to be the shape of that product.

Further, depending on the size of the store, retailers allocate one planogram for each type of commodity. Within a commodity type, SKUs can be clustered in multiple hierarchies, based on their types, brands, size, taste, etc. To reduce customer search effort, retailers commonly allocate each hierarchy level of SKUs in a rectangular area, and all SKUs in one level should respect the boundaries defined by the upper-level hierarchy. For example, in a planogram designated for pet-food, customers do not expect to see food for cats and birds mixed up on the same shelf. This study assumes two-level hierarchy; sub-commodity (e.g., cat and bird) and SKU. Rectangular area allocation requires facings of SKUs and SKUs of sub-commodities to be adjacent in the horizontal or vertical direction.

Parameters and decision variables used in the JSD-SSA model are summarized in Tables 2 and 3.

Table 2. Sets and parameters

Notation	Definition
$I \equiv \{1,2,3, \ldots, \mathrm{N}\}$	Set of SKU; $i, j \in I$
$F \equiv \{1,2,3, \ldots, \mathrm{R}\}$	Set of family; $f, g \in F$
$K \equiv \{1,2,3, \ldots, m\}$	Set of shelves; $k, p \in K$
PW, PH	Planogram length/height (in inches)
P_i	Price of SKU i (in $)
L_i, D_i	Minimum, maximum number of facing for SKU i
W_i, H_i	Length/height of SKU i (in inches)
Z_i, E_i	Maximum face length/height allocation for SKU i
T_{if}	1 if SKU i is a member of family f; 0, otherwise
S^-, S^+	Minimum and maximum number of shelves
H^-, H^+	Minimum and maximum shelf height
W^-, W^+	Minimum and maximum shelf length
VS, VF	Tolerance length for SKU and family alignment

Table 3. Decision variables

Notation	Definition
m	Number of shelves
sx_k, sy_k	x/y coordinate of the left/bottom corner of shelf k
sh_k, sw_k	Height/length of shelf k (in inches)
t^x_{kp}, t^y_{kp}	1, if shelf k is strictly to the east/north of shelf p; 0, otherwise
x_{ik}, y_{ik}	x/y coordinate of the left/bottom corner of the SKU i on shelf k
z_{ij}	1, if SKU i is strictly to the east of SKU j; 0, otherwise
s_{ik}	1, if SKU i is allocated on shelf k; 0, otherwise.
w_{ik}	Number of faces of SKU i on shelf k
u_i, b_i	Top/bottom shelf of SKU i
v_{fk}	1, if family f is allocated on shelf k; 0, otherwise
l_{fk}, r_{fk}	Left/right coordinate of family f on shelf k
fu_f, fb_f	Top/bottom shelf of family f

The objective function is to maximize the total revenue across all SKUs for the retailer. This objective function is similar to Yang & Chen (1999), where we use a linear model whereby the visual location effect in the vertical direction is uniform and that the upper bound for demand can be approximated by using historical point of sales data (which defines the maximum number of facings for each SKU).

Maximize $\sum_i \sum_k P_i w_{ik}$ (1)

Subject to

Shelf design constraints

$sx_k + sw_k \leq PW$	$\forall k$	(2)
$sy_k + sh_k \leq PH$	$\forall k$	(3)
$sx_k + sw_k \leq sx_p + PW\left(1 - t_{k,p}^x\right)$	$\forall (k,p), k \neq p$	(4)
$sy_k + sh_k \leq sy_p + PH\left(1 - t_{k,p}^y\right)$	$\forall (k,p), k \neq p$	(5)
$t_{k,p}^x + t_{p,k}^x + t_{k,p}^y + t_{p,k}^y \geq 1$	$\forall (k,p), k < p$	(6)

Shelf design constraints (2)-(6) are similar to facility layout design constraints used in Montreuil (1991) and Heragu & Kusiak (1991). Specifically, constraints (2-3) ensure that all shelves are allocated within the planogram area, while constraints (4-6) ensure that shelf areas do not overlap.

SKU allocation constraints

$L_i \leq \sum_k w_{ik} \leq D_i$	$\forall i$	(7)
$w_{ik} = 0$	$\forall i, \forall k : H_i > sh_k$	(8)
$\sum_i (w_{ik} W_i) \leq sw_k$	$\forall k$	(9)
$w_{ik} W_i \leq Z_i$	$\forall i, \forall k$	(10)
$w_{ik} - M s_{ik} \leq 0$	$\forall i, \forall k$	(11)
$w_{ik} - s_{ik} \geq 0$	$\forall i, \forall k$	(12)
$\sum_i s_{ik} \geq 1$	$\forall k$	(13)
$x_{ik} \geq s_{ik} sx_k$	$\forall i, \forall k$	(14)
$x_{ik} + w_{ik} W_i \leq sx_k + sw_k$	$\forall i, \forall k$	(15)
$y_{ik} = s_{ik}\, sy_k$	$\forall i, \forall k$	(16)
$x_{ik} + w_{ik} W_i \leq x_{jk} + sw_k\left(1 - z_{ij}\right)$	$\forall k, \forall (i,j), i \neq j : s_{ik} + s_{jk} > 1$	(17)
$z_{ij} + z_{ji} = 1$	$\forall (i,j), i \neq j : s_{ik} + s_{jk} > 1$	(18)
$x_{ik} - x_{ip} \leq VS$	$\forall (k,p), k \neq p, \forall i : s_{ik} + s_{ip} > 1$	(19)
$x_{ip} - x_{ik} \leq VS$	$\forall (k,p), k \neq p, \forall i : s_{ik} + s_{ip} > 1$	(20)
$w_{ik} - w_{ip} \leq 1$	$\forall (k,p), k \neq p, \forall i : s_{ik} + s_{ip} > 1$	(21)
$w_{ip} - w_{ik} \leq 1$	$\forall (k,p), k \neq p, \forall i : s_{ik} + s_{ip} > 1$	(22)
$s_{ik} = 1$	$\forall i, \forall k : b_i \leq sy_k \leq t_i \wedge \sim (sx_k + sw_k < x_{ik} \wedge x_{ik} + w_{ik} W_i < sx_k)$	(23)
$b_i \leq PH - (PH - y_{ik} s_{ik})$	$\forall i, \forall k$	(24)
$u_i = max\{s_{ik} sy_k : k \in K\}$	$\forall i$	(25)
$u_i \geq b_i$	$\forall i$	(26)
$u_i - b_i \leq \mathrm{E}_i$	$\forall i$	(27)

Constraints (7) define bounds for the total number of facings for each SKU. Constraints (8) and (9) ensure that an SKU's height/total length complies with its shelf height/length. We control the maximum horizontal/vertical SKU allocation length by using constraints (10) and (27). Constraints (11) and (12) state that an SKU can have facings only on its allocated shelves. Constraints (13) guarantee that all SKUs are allocated. Constraints (14) and (15) determine coordinates of SKUs. Constraints (17) and (18) ensure that SKU areas do not overlap. If facings of an SKU spread over multiple shelves constraints (19) – (22) ensure left and right alignment with a given tolerance. Constraints (23) guarantee vertical adjacency for SKU faces. Constraints (24) - (26) define top/bottom shelf coordinates.

Family constraints

$\sum_i\left(T_{if} s_{ik}\right) - Mv_{fk} \leq 0$	$\forall f, \forall k$	(28)
$\sum_i\left(T_{if} s_{ik}\right) - v_{fk} \geq 0$	$\forall f, \forall k$	(29)
$l_{fk} \leq x_{ik} + (1 - s_{ik})\, PW$	$\forall i, \forall f, \forall k\colon T_{if} > 0$	(30)
$r_{fk} \geq x_{ik} + w_{ik}\, W_i$	$\forall i, \forall f, \forall k\colon T_{if} > 0$	(31)
$r_{fk} - l_{fk} = \sum_i\left(w_{ik}\, W_i\, T_{if}\right)$	$\forall f, \forall k$	(32)
$fu_f = max\left\{t_i\colon i \in F_f\right\}$	$\forall f$	(33)
$fb_f = min\left\{PH - (PH - b_i) : i \in F_f\right\}$	$\forall f$	(34)
$fu_f \geq fb_f$	$\forall f$	(35)
$v_{fk} = 1$	$\forall f, \forall k: \ fb_f \leq sy_k \leq fu_f \wedge$ $\sim (sx_k + sw_k < lf_k \wedge rf_k < sx_k)$	(36)
$l_{fk} - l_{fp} \leq V\mathrm{F}$	$\forall (k,p), k \neq p, \forall f : v_{fk} + v_{fp} > 1$	(37)
$l_{fp} - l_{fk} \leq V\mathrm{F}$	$\forall (k,p), k \neq p, \forall f : v_{fk} + v_{fp} > 1$	(38)
$r_{fk} - r_{fp} \leq V\mathrm{F}$	$\forall (k,p), k \neq p, \forall f : v_{fk} + v_{fp} > 1$	(39)
$r_{fp} - r_{fk} \leq V\mathrm{F}$	$\forall (k,p), k \neq p, \forall f : v_{fk} + v_{fp} > 1$	(40)

Constraints (28) and (29) state that an SKU can have facings on a shelf only if its family is also allocated to that shelf. Constraints (30) and (31) define the left and right coordinates of each family. Constraints (32) ensure SKU allocation is within the family area. Constraints (33) – (35) define top and bottom coordinates of family areas. Constraints (36) guarantee vertical adjacency of SKU faces within each family. Constraints (37) - (40) ensure the left and right alignment of family areas with a given tolerance.

Domain constraints

$$S^{-} \leq m \leq S^{+} \tag{41}$$

$$H^{-} \leq sh_k \leq H^{+} \qquad \forall k \tag{42}$$

$$W^{-} \leq sw_k \leq W^{+} \qquad \forall k \tag{43}$$

$$t_{k,p}^{x}, t_{k,p}^{y}, s_{ik}, z_{ij}, v_{fk} \in \{0,1\} \qquad \forall (i,j), \forall (k,p), \forall f \tag{44}$$

$$m, x_{ik}, y_{ik}, sx_k, sy_k, sw_k, sh_k, l_{fk}, r_{fk}, w_{ik}, u_i, b_i, fu_f, fb_f \in \mathbb{Z}^{+} \qquad \forall i, \forall k, \forall f \tag{45}$$

Constraints (41) – (45) define the domain of each decision variable.

It is worth noting that the linear shelf space allocation is similar to an MKP, which is NP-hard (Yang & Chen, 1999; Bai & Kendall, 2005; J. M. Hansen et al., 2010; Gajjar & Adil, 2011; Geismar et al., 2015). Additionally, the SSA problem is a special case of the facility layout problem, which is also NP-complete (Heragu & Kusiak, 1991). Consequently, the JSD-SSA, which solves product allocation and shelf allocation decisions simultaneously, turns out to be NP-hard as well. So, while small problem instances can be solved optimally using an off-the-shelf commercial solver, realistic problem instances are too large to be solved efficiently; the preliminary test results of the JSD-SSA model on real-world retail data show that it is not possible to get a feasible solution within a reasonable time. To address this issue, we provide a decomposition-based approach, where we combine a Constraint Programming with Particle Swarm Optimization (a population-based metaheuristic) to find near-optimal solutions to large problem instances.

4. A HYBRID DECOMPOSITION-BASED APPROACH FOR JSD-SSA PROBLEM

In order to solve practical cases, we assume that families do not share shelves, therefore we create shelves for each family separately. Our proposed approach decomposes the original problem into two subproblems; (i) partition the planogram area while considering family constraints and (ii) solve the reduced JSD-SSA model for each partition. Essentially, subproblem (i) serves as a controller that identifies candidate partitions of the planogram where families will be allocated, and subproblem (ii) serves as a follower which determines the best design of shelves and assignment of SKUs for each partition.

Because many sets of planogram partitions may need to be evaluated effectively, we leverage the benefits of a population-based metaheuristic, Particle Swarm Optimization (PSO), to solve subproblem (i). Accordingly, we assign a feasible partition to each particle and then solve subproblem (ii) for each corresponding particle to achieve a complete solution to the original problem. For subproblem (ii), we opted for a Constraint Programming (CP) solver as a viable alternative that uses the mathematical model presented in Section 3. Fig. 3 provides a schematic of the decomposition-based approach.

The PSO and CP algorithms interact in the following manner. Each particle in the PSO identifies a rectangular area for each family by partitioning the planogram area, and then evaluating each partition using a feasibility routine (see Section 4.1.2). If the rectangular area is not feasible, then the particle returns a penalty; otherwise, it forwards this solution to subproblem (ii) solved by using the CP. If the CP-based solution is unable to find a feasible solution within a predetermined time, then the particle returns a penalty, otherwise, it returns the objective function value reported by the CP solver. Finally, each particle aggregates all objective function or penalty values reported by each family and reports it to PSO. This information is used by the PSO to update each particle's position and velocity. We use Shi & Eberhart's (1998) speed and position updating functions which consider inertia weight. We now present details for each of these subproblems and the corresponding algorithm below.

4.1. Subproblem (i): PSO-based planogram partitioning

The PSO was introduced by Kennedy & Eberhart (1995), which was inspired by the flock of birds/school of fish, where each bird aims to do one task and can communicate with other birds in the flock. PSO has been successfully implemented in layout optimization literature (Ozcan & Esnaf, 2011, 2016; Mowrey et al., 2018; Guthrie & Parikh, 2020).

As shown in Figure 2, in our PSO implementation, each particle represents a partition of the planogram area as rectangles. The rectangular shapes that represent family areas are partitions of the planogram area and generated by using a guillotine cuts routine.

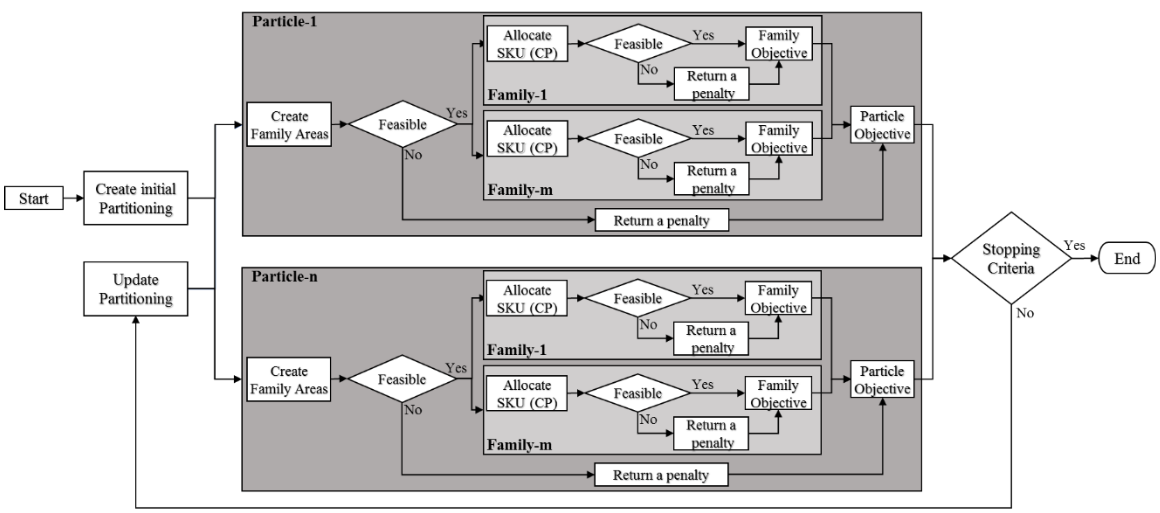

Figure 2. The schematic of the hybrid decomposition-based PSO-CP approach

4.1.1. Guillotine cut algorithm and PSO solution representation

A Guillotine cut (G-cut) slices a rectangle from one edge to another linearly and creates two smaller rectangles. Let M represent the number of families and G represent the number of cuts. To generate M rectangles corresponding to M families, we need G=M-1 cuts. We represent a

PSO solution using 3G random numbers between 0 and 1 as follows: (i) the first G numbers define the cut-direction; if a number in this group is less than or equal to 0.5 then we apply a horizontal cut otherwise a vertical cut; (ii) the second G numbers represent the cut percentage; (iii) the next G-1 numbers determine the rectangle selection; and (iv) the last number is used to assign the families to rectangles. The G-cut algorithm iteratively selects a rectangle and applies a cut. See Figure 3 for an example where we allocate M=3 families (A, B, and C) to a 6 by 8 feet planogram.

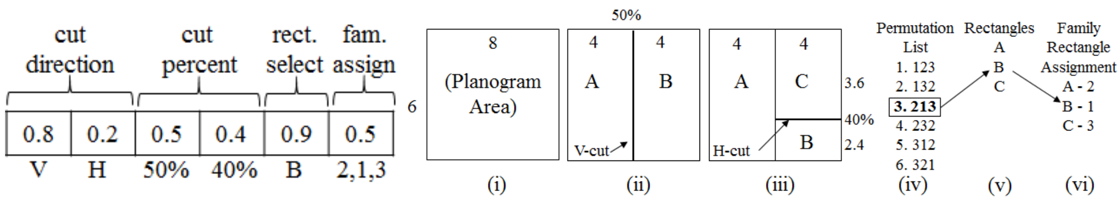

a. Solution representation b. Corresponding partitions

Figure 3. A solution representation and partitioning for a 3-family planogram

Consider in Figure 3.a a potential solution corresponding to a particle in the PSO derived from the G-cut. In this example, there are 3 families and we apply two cuts. For the first cut, we use the 1st and the 3rd numbers (0.8 and 0.5). Here 0.8 represents the vertical cut, while 0.5 represents the cut percentage on the horizontal edge and determines the cut distance from the origin. We use the lower left corner of each rectangle as the origin. Initially there is one rectangle (Fig.3.b.i); we maintain a list of rectangles (Fig. 3.b.v). As we apply cuts, we create new rectangles and add them to the list. After the first cut, we have 2 rectangles (Fig. 3.b.ii). For the second cut, first, we use the 5th number (0.9) to select a rectangle from the list. In this example, we multiply 2 (number of rectangles) by the 5th number (0.9) and round the result, which equals 2. As a result, we select the second rectangle (B) for the second cut. Then we apply the second cut to rectangle B, by using the 2nd and 4th numbers (0.2 and 0.4). Subsequently, we slice rectangle B horizontally at y-coordinate 2.4 and create C (4.b.iii). Next, C is added to the rectangles list and B’s height is updated. Finally, we assign families to rectangles by multiplying the last number in the solution representation (0.5) with the number of permutations (6) and round the result. In this example, we select the 3rd permutation and assign it to rectangles A, B, and C (4.b.vi).

4.1.2. Necessary conditions for feasibility and calculation of penalty

Necessary Conditions: Checking the feasibility of family space allocation (by partitioning the planogram) requires solving the reduced model; however, this process is time-consuming. We, therefore, identified necessary conditions to check the feasibility of the solution and speed up the PSO algorithm. Necessary conditions do not guarantee the feasibility of the entire solution (which includes allocation of SKUs); i.e., space allocation can pass the test, but there may not be any feasible arrangement of SKUs later on. We define a family space allocation solution as infeasible if at least one of the following conditions is met:

a. If any SKU's length is greater than its' family rectangle length or SKU's height is greater than its family rectangle height.
b. If total Lower-Bound Facing Space of SKUs for a given family is greater than that family rectangle space.

Penalty Term: The penalty term guides particles towards a feasible solution. As the solution gets closer to the feasible region, the penalty term gets smaller and inside the feasible region, it disappears. The calculation of the penalty term is given in Eq. 46:

$$\sum_f \sum_i \left(\min\left\{0, sw_f - W_i : i \in F_f\right\} + \min\left\{0, sh_f - H_i : i \in F_f\right\}\right) + \min\left\{0, sw_f sh_f - \sum_{i \in F_f} L_i W_i H_i\right\} \tag{46}$$

Eq. 46 penalizes if the SKU is wider than its family rectangle length or if the SKU is taller than its family rectangle height (first two terms), and if a family's lower bound facing space is greater than its rectangle area (the last term).

4.2. Subproblem (ii): CP-based solution for the reduced problem

Recall that because the family constraints are now handled in subproblem (i), the result which reduced the JSD-SSA problem is what we refer to as subproblem (ii). However, this subproblem is very challenging to solve in a reasonable amount of time. Our initial tests with a commercial solver (CPLEX) suggested that only very small problems (e.g., 3 SKUs, 15" × 15" planogram) can be solved in a reasonable amount of time (380 seconds). For realistic problems that are much larger than that, the CPLEX solver was not able to solve the model within 30 minutes. On the other hand, the CP solver was able to find a high-quality feasible solution in less than 160 seconds. Appendix A provides details of this comparison. We allow the CP solver up to 300 seconds based on the planogram features (size, number of SKU, family, etc.).

To invoke the PSO-CP approach, we created a unique initial solution for each particle. An initial solution is a partitioning of a planogram area that meets all necessary feasibility conditions and minimizes Eq. 46. We solved the partitioning problem using a particle swarm optimization with the guillotine cut solution representation.

Finally, we generated several small problem instances to evaluate the performance of our proposed approach against CPLEX optimal solutions. The findings are summarized below.

4.3. Performance of the proposed approach

We created 13 cases for this comparison. For each case, we randomly selected SKUs from the real-world planogram data and assigned family labels. We executed all cases on a personal computer with an Intel Core TM i-7 8650U CPU, Gen 8 processor system, with a processor clock speed of 1.90 gigahertz and a total of 16 GB RAM. We used IBM CPLEX Studio 12.9.0 CPLEX, while for PSO-CP, we incorporated Python IBM CP solver and pyswarms libraries (James V. Miranda, 2018). All algorithms used 6 cores in parallel. We set the time limit to 12 hours (i.e., 43,200 seconds) for all runs. The final state was recorded upon completion of the running algorithm time limit.

Table 4. The performance of PSO-CP algorithm

#	Case	CPLEX			PSO-CP		
		Best int	Gap (%)	Time (s)	Obj.	% Diff from CPLEX	Time (s)
1	N4F2W14H14	41.3	0	10	41.3	0	1
2	N5F3W15H15	34.3	0	105	34.3	0	1
3	N5F2W24H60	87.2	31.1	43,200	97.27	-11.55	10
4	N5F3W24H60	136.44	40.42	43,200	133	2.52	58
5	N5F5W24H60	42.31	61.47	43,200	42.31	0	82
6	N10F2W36H72	222.59	30.07	43,200	222.59	0	172
7	N10F3W36H72	255.4	15.23	43,200	255.4	0	257
8	N10F5W36H72	379.52	19.15	43,200	391.21	-3.08	580
9	N20F2W60H72	-	-	43,200	315.79	-	1,162
10	N20F3W60H72	-	-	43,200	681.59	-	1,258
11	N20F5W60H72	-	-	43,200	479	-	1,802
12	N50F2W144H72*	-	-	3,726*	1393.53	-	5,011
13	N100F2W192H84*	-	-	29,034*	9872	-	2,597

* Ran out of memory

In Table 4, the column Case employs a notation, where N, F, W, and H represent the number of SKUs, number of families, planogram length, and planogram height, respectively. For example, Case #3 (N5F2W24H60) has 5 SKUs which are clustered into 2 families, planogram length of 24" and height of 60".

A few things are worth observing in Table 4. For cases where CPLEX was able to find an optimal solution, the PSO-CP achieved the same optimal solution in as much as 1% lower time. For all other instances where CPLEX was only able to get the best integer solution, Except for Case #4, PSO-CP either found the best integer reported by CPLEX or better solution, and solution time was 1% of CPLEX solutions. For Case #4, PSO-CP was within 2.52% of the best integer solution reported by CPLEX, and the solution time was 0.13% of those solutions. For all other problems (i.e., Cases #9-#13), PSO-CP was still able to find solutions in a reasonable time.

We further tested the convergence of the PSO-CP approach on small cases. We ran Cases #3, #6, and #7 three times, using 6 particles for 50 iterations. At each iteration, we recorded the objective function value reported by each particle, and at the end of each run we saved the best objective function value reported by each particle and the global best objective function value. At the end of each run, we calculated the Mean Absolute Percentage Error (MAPE) between particles, and after the final run, we calculated MAPE between global best objective function values. The average MAPE between particles was 0.04% and the average MAPE between the global best objective function values was 0.03%. Details of all runs are given in Appendix B.

These experiments suggest that our proposed PSO-CP algorithm appears to converge and perform fairly well compared to solutions obtained via CPLEX. We, therefore, deem this approach as viable to solving realistic problem instances and use it for all subsequent experiments.

5. EXPERIMENTAL STUDY

To better understand how SKU shape variation and the number of family affect planogram design and SKU allocation, we conducted a comprehensive experimental study. We collected actual data from a US retailer. The data included 35,139 planograms from 109 retail stores and 32,399 unique SKUs. We first describe the data we used and analysis we conducted to determine levels of key system parameters (SKU shape variation, and planogram space). Following that, we discuss our findings and practical insights.

5.1. Data generation and data collection

For the shape-variation and planogram space analyses, we compared revenues of planograms by changing the shelf length and height across various levels of SKU shape-variations and planogram sizes. To conduct a meaningful comparison and extract managerial insights, we generated several datasets using the patterns in the real planogram designs available to us. We first represented SKU profit as profit per square-inch (PPI). By using a fixed PPI value and planogram space, we ensure that the upper bound of total revenue derived from a given planogram remained unchanged across different assortments.

5.2. SKU shape variation

To incorporate the effect of SKU shape variation on planogram design, we first devised a metric to measure the shape variation. For clustering purposes, we selected a feature that is properly distributed within an upper and lower bound. Therefore, we use Major

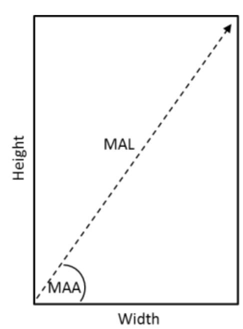

$$\text{MAA} = \tan^{-1}\left(\frac{height}{width}\right)$$

$$\text{MAL} = \sqrt{width^2 + height^2}$$

Figure 4. MAL and MAA

Axis Angle (MAA) (Wirth, 2004). MAA is bounded between 0 and $\pi/2$. To describe the size of a rectangle we use the Major Axis Length (MAL) (Wirth, 2004); see Figure 4.

For each of the 32,399 SKUs, first, we calculated MAA and MAL metrics and normalized them using z-score (MAA: μ: 0.952, σ: 0.264; MAL: μ: 8.282, σ: 3.848). Then we removed outliers from MAL ($\sigma \geq 5$), which removed SKU's whose MAL values larger than 48 inches. MAA feature did not have any outliers. We illustrate the distribution of each metric and their joint distribution in Figure 5. This figure shows that planograms often have small and tall SKUs; MAAs range between 55° and 65°, and MALs range between 5 and 12 inches.

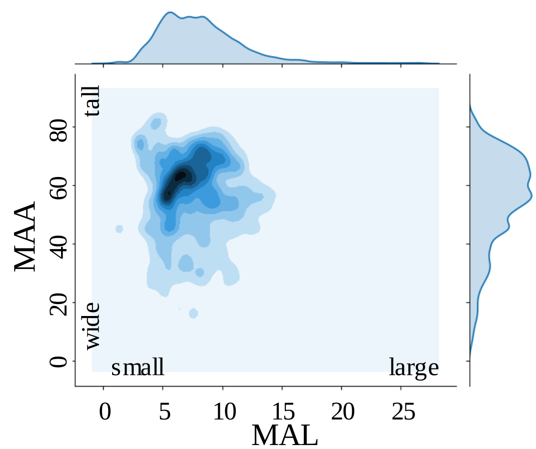

Figure 5. The joint distribution of MAA and MAL

Once we have MAA and MAL for every SKU, we can measure the SKU-shape variation in every family. Because we also allocate families together, measuring SKU-shape variation only within families is not sufficient. Let family A have a unique SKU-shape, and family B have another unique SKU-shape; in this case, the shape variation within each family will be zero, but the shape variation between families can be substantial. We, therefore, need both within and between family cluster distance measurements to better describe the shape variation across families. For this, we employ within-cluster scatter matrix (S_w) and between-cluster scatter matrix S_b per Fukunaga (1990). Because S_w and S_b are matrices, we derive two scalar quantities to measure within- and between-cluster distances; i.e., the trace of S_w (TW) and the trace of $S_w^{-1}S_{b.}$ (TWiB), respectively (Theodoridis & Koutroumbas, 2009).

For shape analyses, if all SKUs share the same size, within and between cluster distances would be 0 (Figure 6.a); we refer to such planograms with low TW and TWiB values as 'homogeneous.' If shapes of SKUs are all very different from each other, then we will observe high within cluster and low between cluster distances (Figure 6.b); we call such planograms with high TW and low TWiB as 'heterogeneous.' Finally, if SKU shapes within families are the same, but different between families, then we observe 'less homogeneity/heterogeneity.' Under these conditions, we expect to have low within cluster distance and high between cluster distances (Figure 6.c); i.e., low TW and high TWiB.

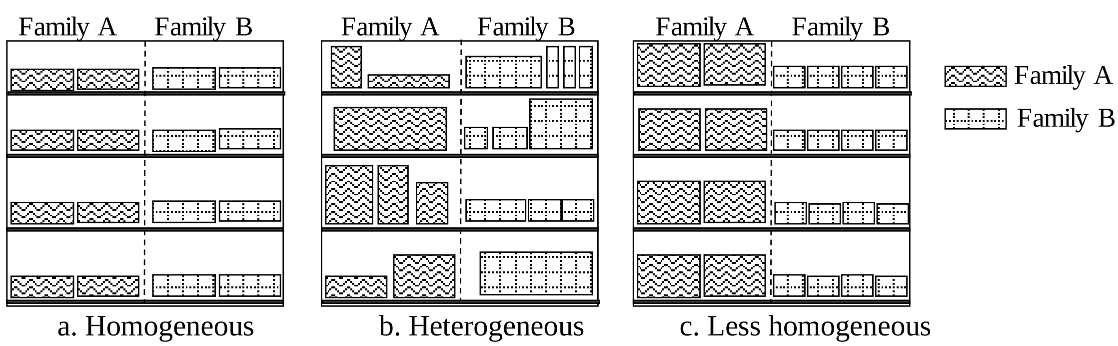

Figure 6. Homogeneity/Heterogeneity of clusters

We utilized 35,139 planogram data and calculated TW and TWiB values for each planogram. We used clusterCrit (version 1.2.8) library in R programming language for calculations and we refer to (Desgraupes, 2018) for the implementation details of TW and TWiB.

Finally, we applied the 2-dimensional K-means clustering algorithm on the joint distribution of TW and TWiB to cluster planograms into 3 categories; homogeneous, heterogeneous, less homogeneous (Figure 7).

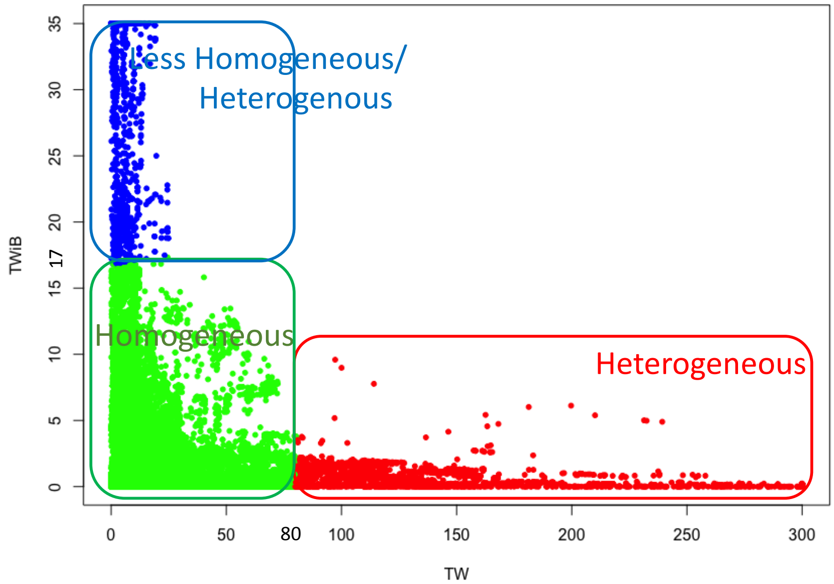

Figure 7. 2D k-means clustering of TW and TWiB

In Figure 7, X-axis represents TW, Y-axis represents TWiB, and each point represents one planogram. The clusters are labeled with colors. We classify a planogram as:

- homogeneous, if its TW < 17 and TWiB < 80
- heterogeneous, if its TW ≥ 80 and TWiB < 17
- less homogeneous/heterogeneous, if its TW < 80 and TWiB ≥ 17

5.2. Space fitness

Since planograms come in different sizes, we cannot compare revenues across different planograms. Therefore, we propose the Space Fitness (SF) (Eq. 47) metric as the ratio of the total Lower-Bound Facing Space (LFS) (Eq. 48) to the planogram space. By using SF, we can classify the space of a planogram as tight, fit, or loose. As SF gets closer to 1, planogram space becomes tighter, and SKUs lose their extra facings. Also, as SF approaches zero, the planogram space becomes looser, and assigning SKU facings becomes straightforward. Note that SF>1 means there is not enough space on the planogram to even assign the minimum facings to each SKU; we do not consider such cases in our experiments.

$$Space\ Fitness = \frac{LFS}{PW * PH} \tag{47}$$

$$LFS = \sum_i W_i H_i \, L_i \tag{48}$$

We generated 4 instances (A-D) of Homogeneous (HM), Less-homogeneous (LHM), and Heterogeneous (HT) planograms. Then, we created 4 different planogram spaces and tested each instance with them. For this, we kept the planogram height at 60 in. and used 60, 72, 84, and 106 in. planogram lengths. The corresponding SF values of these planogram spaces were 0.28, 0.23, 0.20, and 0.16. The resulting experiment design is summarized in Table 5.

Table 5. Experiment design factors and levels

Factors	Levels								
		A		*B*		*C*		*D*	
		TW	*TWiB*	*TW*	*TWiB*	*TW*	*TWiB*	*TW*	*TWiB*
Shape Variation	HM	0	0	1	9.3	3	5.3	0.2	3.2
	LHM	0.4	INF	4.6	24.8	39.6	24.7	18.1	16.7
	HT	96.5	0.42	166	0.26	268	0.8	309	0.22
Space Fitness (SF)	0.28, 0.23, 0.20, 0.16 (PH: 60”, PW: [60, 72, 84, 106])								
Shelf length	12”, 24”, 36”, 48”, 60“								

We present run times and objective function values in Appendix C. For our analyses, we compare the revenues of each instance by using revenue increase ratio (RIR), which is the ratio of revenue corresponding to an alternative shelf length with that of a 60” shelf length. We present the resulting revenue ratios in Table 6.

Table 6. RIR across various experimental settings

Case	TW	TWiB	*SF* = 0.28 (PW:60, PH:60)					*SF* = 0.23 (PW:72, PH:60)					*SF* = 0.20 (PW:84, PH:60)					*SF* = 0.16 (PW:106, PH:60)				
			Min Shelf Length					*Min Shelf Length*					*Min Shelf Length*					*Min Shelf Length*				
			12	24	36	48	60	12	24	36	48	60	12	24	36	48	60	12	24	36	48	60
HM-A	0	0	1	1	1	1	1	1	1	1	1	1	1	1	1	1	1	1	1	1	1	1
HM-B	1	9.3	1.023	1.020	1	1	1	1.006	1.003	1	1	1	1.012	1	1	1	1	1.002	1.002	1	1	1
HM-C	3	5.3	1	1	1	1	1	1	1	1	1	1	1	1	1	1	1	1	1	1	1	1
HM-D	0.2	3.2	1	1	1	1	1	1	1	1	1	1	1	1	1	1	1	1	1	1	1	1
LHM-A	0.4	INF	1.091	1.091	1	1	1	1.078	1.065	1.065	1	1	1.022	1.011	1	1	1	1	1	1	1	1
LHM-B	4.6	24.8	1.026	1.023	1	1	1	1.061	1.032	1.007	1	1	1.070	1.061	1.053	1	1	1.043	1.029	1.016	1.013	1
LHM-C	39.6	24.7	1.008	1.008	1	1	1	1.061	1.000	1.000	1	1	1.041	1.033	1.025	1	1	1.019	1.019	1.019	1.019	1
LHM-D	18.1	16.7	1.064	1.023	1	1	1	1.029	1.027	1.026	1	1	1.015	1.015	1.011	1	1	1.083	1.019	1.022	1.022	1
HT-A	96.5	0.42	1.545	1.541	1	1	1	1.406	1.394	1.381	1	1	1.361	1.336	1.318	1	1	1.296	1.271	1.277	1.269	1
HT-B	166	0.26	1.121	1.088	1	1	1	1.131	1.100	1.093	1	1	1.109	1.098	1.068	1	1	1.046	1.032	1.010	1.010	1
HT-C	268	0.8	1.132	1.092	1	1	1	1.120	1.106	1.038	1	1	1.064	1.055	1.032	1	1	1.095	1.097	1.073	1.072	1
HT-D	309	0.22	1.093	1.085	1	1	1	1.098	1.076	1.038	1	1	1.094	1.070	1.063	1	1	1.157	1.143	1.130	1.038	1

We summarized Table 6 by averaging RIR-values of shape variation and space fitness combinations and displayed results in Table 7.

Table 7. Average RIR over 60”-shelf length

Shape Variation			*MSL 48”*	*MSL 36”*			*MSL 24”*				*MSL 12”*			
	TW	TWiB	SF	SF			SF				SF			
			0.28	0.28	0.23	0.2	0.28	0.23	0.2	0.16	0.28	0.23	0.2	0.16
HM	1.1	4.5	1	1	1	1	1.01	1	1	1	1.01	1	1	1
LHM	15.7	22.1	1.01	1.02	1.02	1.01	1.04	1.03	1.03	1.02	1.05	1.05	1.04	1.04
HT	210	0.4	1.01	1.14	1.12	1.12	1.2	1.17	1.14	1.14	1.22	1.19	1.16	1.15

Figure 8 displays a 3D representation of Table 7.

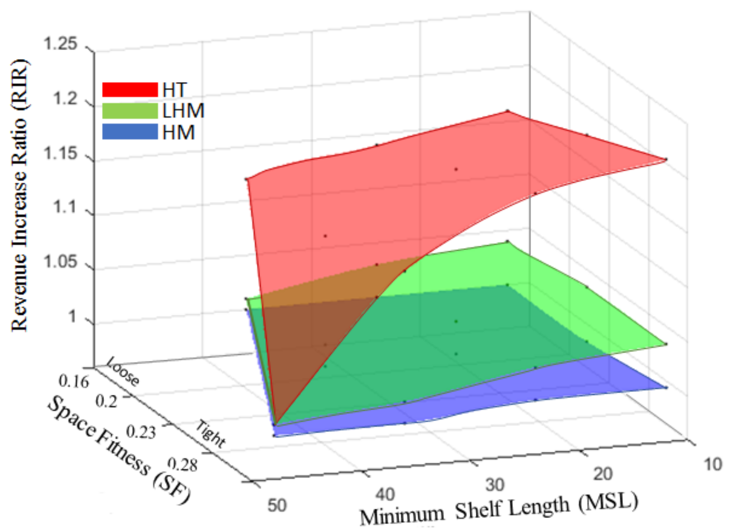

Figure 8. Change in RIR with respect to SF and shape variation across various shelf lengths

In Figure 8, X, Y, and Z-axes represent MSL, SF, and RIR respectively. RIRs are colored by their shape variation levels. The planogram instance in the lower-left corner (tight space, 48” MSL) can be considered as an improved version of the classic SSA layout optimization problem, where shelf heights and the number of shelves are additionally considered. Layers in Figure 8 reveal that the JSD-SSA model improves the revenue significantly based on the shape variation. More specifically, the JSD-SSA model improved the revenue on average 22% for heterogeneous, 20% for less-homogeneous, and 1% for homogeneous planograms.

Observation 1: Higher within family variation in SKU shapes induces the need for a customized shelf design.

Recall that TW, which indicated the within-family variation, increases as within-family shape variation increases (see Table 7). Except for the HM row in Table 7 (within-family shape variation is negligible), all RIR values increase as TW values increase. This can also be observed in Figure 8; for higher shape variations we observe higher revenue increase ratios (LHM and HM layers). Across all shape fitness values, we observe substantial benefits in RIR (up to 22%) through customized shelf design. If SKU families have both very thin-tall and wide-short SKUs, then the benefits of a customized shelf design are much higher.

To understand the underlying reasons, consider the Case HT-A for SF=0.28 for a planogram with height and length are 60” (area = 3600 $inch^2$) from Table 6. The two solutions, one corresponding to a traditional shelf design (all shelves 60”) and the other corresponding to a customized design are shown in Figure 9.a and b. A total of 23 facings of SKUs were allocated in the traditional design, whereas the customized shelf design allocated 43 facings. As a result, the traditional shelf design had 1362 $inch^2$ unutilized space compared to only 143 $inch^2$ in the customized design. For the traditional shelf design, the given planogram and SKU dimensions limited the allocation of another 60”-shelf. Therefore, SKUs with different heights were allocated together on the same shelf. However, the customized shelf design improved the shelf layout by grouping SKU with similar shapes on smaller shelves. As a result, new facings were allocated to the unutilized space next to bigger SKUs. Both planograms share the same size, hence while traditional shelf design generated $2,238, the customized one generated $3,457, which is a 54.4% increase in revenue.

SKU	W	H	Family
0	2	19	0
1	8	17	0
2	8	19	1
3	3	18	2
4	17	4	0
5	4	16	1
6	16	5	1
7	7	10	1
8	11	3	0
9	10	20	2
10	12	5	1
11	15	3	0

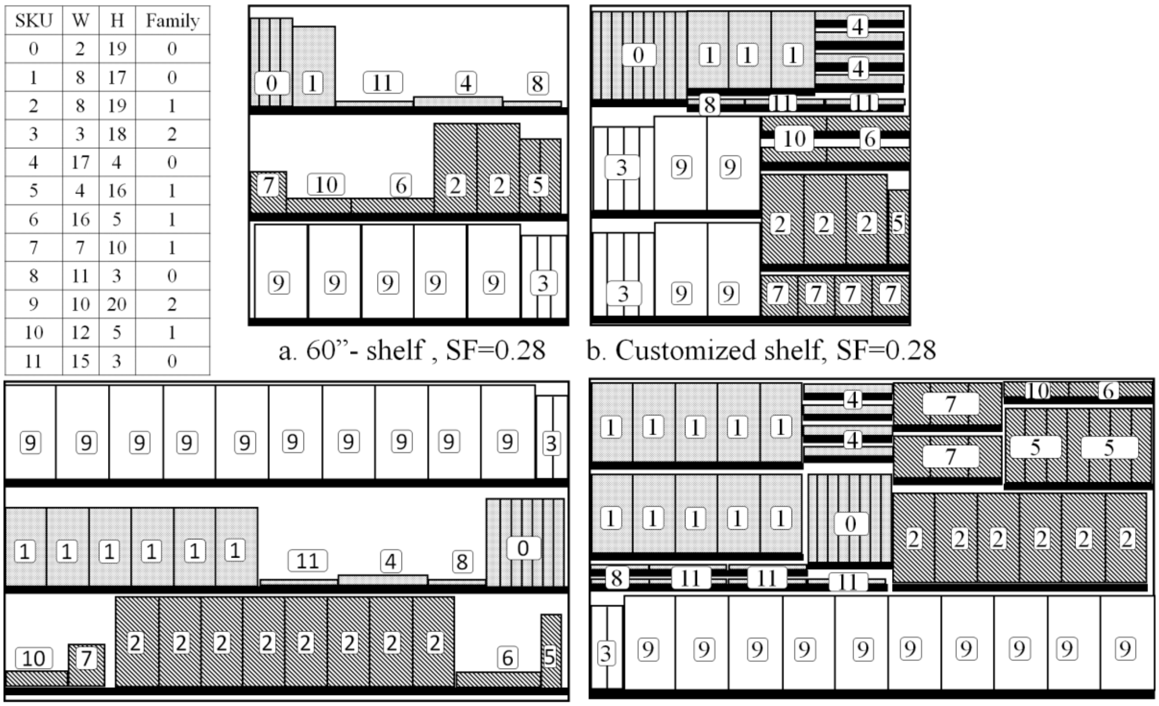

a. 60”- shelf , SF=0.28 b. Customized shelf, SF=0.28

c. 60”- shelf , SF=0.16 d. Customized shelf, SF=0.16

Figure 9. SKU arrangement in 60”-shelf and customized shelf designs for SF=0.28 and SF=0.16

Observation 2: As the planogram space fitness increases, shorter shelves become more beneficial, especially in heterogeneous cases.

Recall that we use SF (space fitness) to quantify the tightness in space of a planogram. So, in Table 7, across MSL and shape variation values, as SF increases, we observe a general increase in RIR over the 60” shelf length. While for all HM cases, the increase in RIR of shorter shelves can be up to 1% as SF increases, for the HT cases, these benefits can increase up to 22%. This is also evident from Figure 8, where for a fixed point on the Y-axis (SF), we observe a consistent rise in RIR value as we move from left to right on the X-axis (MSL).

To explain this behavior, consider Case HT-A with SF=0.16 and SF=0.28 (in Table 6). For SF=0.28, the planogram dimensions are 60” × 60” (total area = 3,600 inch^2), while for SF=0.16, these are 60” × 106” (total area = 6,360 inch^2) Figure 9.a and c illustrate the solutions generated by our approach for MSL=12” in both cases. The ratio of the unutilized space to the total planogram space in Figure 9.a is 0.37 (1362/3600) for SF=0.28, whereas it is 0.24 (1534/6360) for SF=0.16. Note that, in Figure 9, SKUs 4,6,7,8 and 10 cause unused space. In both SF= 0.28 and SF=0.16 cases for 60"-shelf design, the JSD-SSA model allocates these SKUs at their lower bound facings to minimize the unutilized space, given that PPI equals $1/inch^2. Moreover, in these images, we also observe that SKUs with higher profitability are allocated more, if possible up to their upper bound (SKU 9). Therefore, increasing the planogram space (lowering the SF value) increases the facings of profitable SKUs, while keeping the less profitable SKU facings at their lower bound; hence decreases the ratio of unutilized space. In other words, higher SF values create higher unutilized space ratios, which we eliminate by using the JSD-SSA model.

Observation 3: SKUs in the best layouts seem to have a common factor or multiple with other SKUs and planogram dimensions.

Our results suggested that an allocation of SKUs sharing a common factor or multiple with the planogram dimensions tend to utilize the planogram space better. To better understand the common factor, consider height×length of SKUs A and B as 3"×5” and 9"×5”, and that of the planogram as 9”×10". Because SKUs and the planogram heights share a common factor (3") in height, the planogram space can be used thoroughly by creating 3 shelves on top of each other for SKU A and a shelf for B next to SKU-A. Now if SKUs do not share a common factor, the planogram space can still be completely utilized if they share a common multiple. For instance, consider height×length of SKUs A and C as 3"×5” and 5"×5”, and that of the planogram as 15”×10". These SKUs and planogram do not share a common factor, but they share a common multiple (15"); this results in a design with 5 shelves for SKU A on top of each other and 3 shelves for SKU B on top of each other (next to SKU A), together covering the entire planogram space. Figure 10 shows the generated planograms for LHM-A and HT-C cases with MSL 12”. Both LHM-

A and HT-C have 12 SKUs and 3 families and planogram length, and height is set to 60" and the total area is 3600 inch^2. Notice that LHM-A has SKU lengths and heights, as well as the planogram length and height, have a common factor of 5 and a common multiple of 30; this is not the case for HT-C case.

SKU	W	H	Family
0	10	10	0
1	10	10	0
2	10	10	0
3	10	10	0
4	5	30	1
5	5	30	1
6	5	10	2
7	10	5	2
8	10	5	2
9	10	5	2
10	10	5	2
11	10	5	2

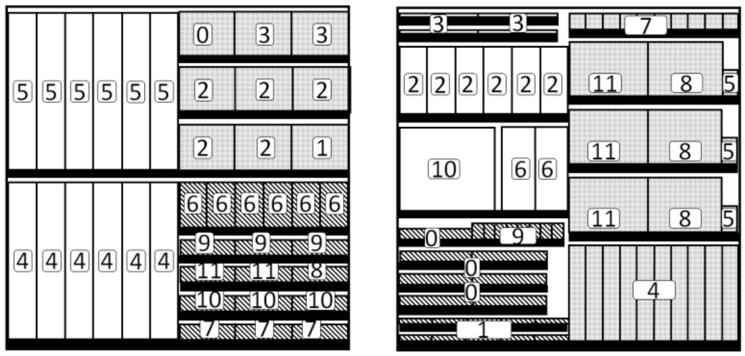

SKU	W	H	Family
0	13	4	1
1	6	3	1
2	5	14	0
3	14	3	0
4	3	19	2
5	3	7	2
6	6	17	0
7	3	5	2
8	13	12	2
9	2	5	1
10	17	17	0
11	14	12	2

a. LHM-A solution b. HT-C solution

Figure 10. Factors and multiples

The LHM-A solution used all space and generated a maximum revenue of \$3600. The common factor among the SKUs and planograms dimensions was 5. In contrast, the solution for HT-C (with no clear common factor) resulted in 119 inch^2 unutilized space and generated \$3481 revenue. Specifically, SKUs 4, 5, 7, 8, and 11 were well-aligned vertically, but not horizontally, causing 45 inch^2 space as unused. Lengths of SKUs 2, 3, 6, and 10 did not have a common multiple that is smaller than the overall planogram length, as a result, 25 inch^2 space was unused. The length of SKU 0 was a prime number, clearly resulting in a vertical misalignment; 13 inch^2 remained unused. Also due to the height difference between SKU 0 and 9, 13 inch^2 area could not be utilized.

These results show that if the dimensions of SKUs do not have a common factor or multiple, some space tends to stay unutilized. This insight can be useful for retailers for assortment selection decisions and for negotiating with suppliers on the product packaging as that may affect planogram space utilization, and thus profitability.

6. CASE STUDY

To illustrate the use of our approach, we considered a real planogram at a store of a leading US retailer in our region and attempted to improve it by using our JSD-SSA model. This existing planogram has 55 SKUs related to diabetic care, grouped into four families. The price, dimension, family, and the facings of each SKUs are given in Appendix D. The within and between shape variations of the planogram are 1067.47 and 1.78. Accordingly, per Chapter 5, we classify this diabetic care planogram as heterogeneous. The height and width of planogram space are 37” and 52”, respectively, and the LFS is 1029 inch^2. The corresponding SF then is 0.53, which is tighter than all our experimental cases. Figure 11 represents the current and improved layouts for the diabetic care planogram.

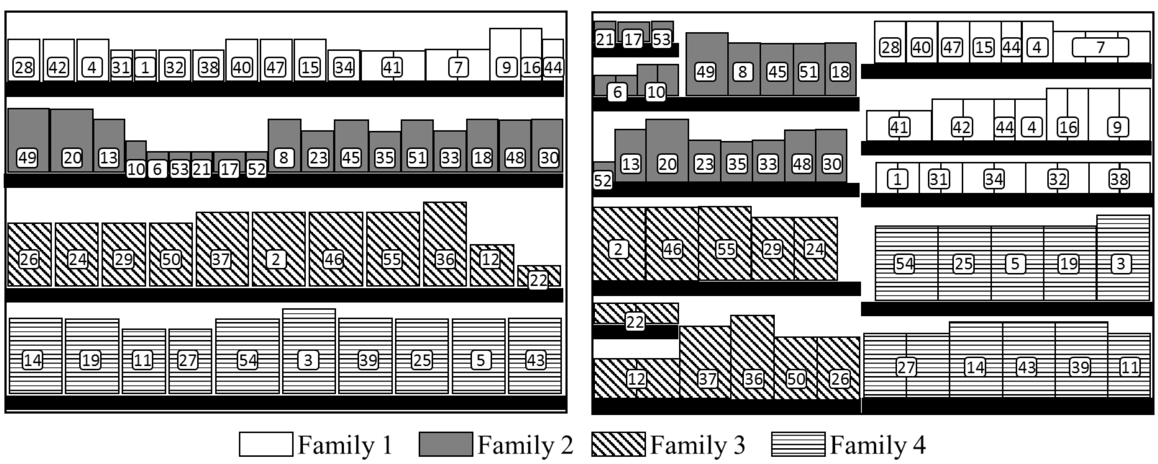

a. Current planogram　　　　b. Improved planogram

Figure 11. Shelf design and SKU position for the two planograms

In the current planogram (Figure 11.a), all SKUs have one facing, except for 2 SKUs who have facings. That is, there are a total of 57 faces. The estimated revenue from this planogram is \$897.9 and the unused space ratio is 0.284.

To improve this current planogram, we set the lower bound of facings for all SKUs to 1 and upper bound to 1 more than the current facings. An improved planogram using our PSO-CP approach is illustrated in Figure 11.b. A few key observations for the improved planogram follow:

- The current planogram uses four 52” shelves, whereas the improved planogram uses five 27” shelves, four 25” shelves, and two 8” shelves. While each family in the current planogram is assigned on one shelf and distributed vertically, shorter shelves allow better partitioning of the planogram area in the improved version.

The improved planogram increased the number of SKU faces from 57 to 74 and reduced the unused space ratio from 0.284 to 0.16 (without reducing the current number of faces). Because the planogram space fitness value is high (i.e., tight) more facings were assigned to smaller sized SKUs than larger. The resulting increase in the revenue is 29.2% (from $897.9 to $1160.2). Additional details can be found in Appendix D.

7. CONCLUSION AND FUTURE RESEARCH

Configurable shelves are becoming prominent among a variety of retailers. Configurable shelves offer retailers the freedom of allocating various sized products together without wasting the valuable shelf space. This capability can bring competitive advantage to retailers, by enabling them to create richer assortments within a smaller planogram space. However, it is unclear how such shelves should be optimally designed and the impact of various product-related factors that affect such designs.

To this extent, we proposed an optimization-based approach for the joint shelf design and shelf space allocation problem with the objective of designing a customized shelf layout that maximizes the space-utilization and revenue. Because of the problem complexity, we resorted to a decomposition-based approach where we first solve the family area allocation problem (using particle swarm optimization) and then the SKU assignment problem per family (via Constraint Programming). In so doing, we proposed a metric to measure the degree of shape diversity of products and gave guidelines and thresholds for classifying assortments.

Retailers and other industries that allocate items on a storage area, intuitively know that diversity of shapes requires adjustment of dimension and position of storage units, such as shelves, bins. One key finding of our study is, it exposes the relation between shape variation, shelf length, available space, and revenue. Increasing the within-family shape variation can result in higher revenue increase ratios. Our experiments suggest that for non-homogeneous planograms, customized shelf designs can increase the revenue can by 22%, based on within family SKU shape variation level. Through our experiment, we showed that as the space fitness increases the benefits gained from a customized shelf design also increase. Further, better layout results can be obtained if assortments were constructed in a way that dimensions of SKUs share a common multiple or factor with both other SKUs and the planogram space. Especially, we observed that avoiding SKUs with prime number dimensions can reduce the unutilized space, as they fail to align well with other SKUs.

While our model can handle gondola, peg, bin, and mixed type of shelving, there is room for further enhancements. First, incorporating vertical and horizontal location effects of an SKU on customer demand will allow further exploration of the choice of shelf length at each height level and across the length of the planogram. However, the location effect functions proposed in the existing literature are nonlinear, and so will add to the complexity of the model. Second, while we considered that the SKU dimensions provided to us already considered stacking within that SKU, it is possible to explicitly include them as decision variables in the model. This will allow further exploration of the effect of various SKU orientations and stacking levels on the choice of shelf lengths and overall planogram design. Our study considers a 2-level family hierarchy. We believe the JSD-SSA model can be improved to handle any generic hierarchy structure by borrowing the modeling approach of Bianchi-Aguiar et al. (2018). It would be interesting to see how location effects and inventory decisions would impact the shelf design and revenue. Another interesting extension to our model would be adding the proximity impact on demand for compatible products. However, introducing these extensions brings more complexity, and we believe that there is a lot of room for improving the heuristic method for dealing with complexities.

REFERENCES

1. Bai, R., & Kendall, G. (2005). An Investigation of Automated Planograms Using a Simulated Annealing Based Hyper-Heuristic. In *Metaheuristics: Progress as Real Problem Solvers* (pp. 87–108). https://doi.org/10.1007/0-387-25383-1_4
2. Bai, R., & Kendall, G. (2008). A Model for Fresh Produce Shelf-Space Allocation and Inventory Management with Freshness-Condition-Dependent Demand. *INFORMS Journal on Computing*, *20*(1), 78–85. https://doi.org/10.1287/ijoc.1070.0219
3. Bai, R., van Woensel, T., Kendall, G., & Burke, E. K. (2013). A new model and a hyper-heuristic approach for two-dimensional shelf space allocation. *4OR*, *11*(1), 31–55. https://doi.org/10.1007/s10288-012-0211-2
4. Bianchi-Aguiar, T., Silva, E., Guimarães, L., Carravilla, M. A., & Oliveira, J. F. (2018). Allocating products on shelves under merchandising rules: Multi-level product families with display directions. *Omega*, *76*, 47–62. https://doi.org/10.1016/j.omega.2017.04.002
5. Borin, N., Farris, P. W., & Freeland, J. R. (1994). A Model for Determining Retail Product Category Assortment and Shelf Space Allocation. *Decision Sciences*, *25*(3), 359–384. https://doi.org/10.1111/j.1540-5915.1994.tb00809.x
6. Brown, W., & Tucker, W. T. (1961). The Marketing Center: Vanishing Shelf Space. *Atlanta Economic Review*, *October*, 9–13.
7. Bultez, A., & Naert, P. (1988). SH.A.R.P.: Shelf Allocation for Retailers' Profit. *Marketing Science*, *7*(3), 211–231. https://doi.org/10.1287/mksc.7.3.211
8. Chen, M., & Lin, C. (2007). A data mining approach to product assortment and shelf space allocation. *Expert Systems with Applications*, *32*(4), 976–986.

https://doi.org/10.1016/j.eswa.2006.02.001

9. Corstjens, M., & Doyle, P. (1981). A Model for Optimizing Retail Space Allocations. *Management Science*, *27*(7), 822–833. https://doi.org/10.1287/mnsc.27.7.822
10. Corstjens, M., & Doyle, P. (1983). A Dynamic Model for Strategically Allocating Retail Space. *Journal of the Operational Research Society*, *34*(10), 943–951. https://doi.org/10.1057/jors.1983.207
11. Curhan, R. C. (1972). The Relationship between Shelf Space and Unit Sales in Supermarkets. *Journal of Marketing Research*, *9*(4), 406. https://doi.org/10.2307/3149304
12. Desgraupes, B. (2018, July 26). *CRAN - Package clusterCrit*. https://cran.r-project.org/web/packages/clusterCrit/index.html
13. Drèze, X., Hoch, S. J., & Purk, M. E. (1994). Shelf management and space elasticity. *Journal of Retailing*, *70*(4), 301–326. https://doi.org/10.1016/0022-4359(94)90002-7
14. Flamand, T., Ghoniem, A., Haouari, M., & Maddah, B. (2018). Integrated assortment planning and store-wide shelf space allocation: An optimization-based approach. *Omega*, *81*, 134–149. https://doi.org/10.1016/j.omega.2017.10.006
15. Flamand, T., Ghoniem, A., & Maddah, B. (2016). Promoting impulse buying by allocating retail shelf space to grouped product categories. *Journal of the Operational Research Society*, *67*(7), 953–969. https://doi.org/10.1057/jors.2015.120
16. Frank, R. E., & Massy, W. F. (1970). Shelf Position and Space Effects on Sales. *Journal of Marketing Research*, *7*(1), 59–66. https://doi.org/10.1177/002224377000700107
17. Fukunaga, K. (1990). *Introduction to statistical pattern recognition* (2nd ed.). Academic Press.
18. Gajjar, H. K., & Adil, G. K. (2011). Heuristics for retail shelf space allocation problem with linear profit function. *International Journal of Retail & Distribution Management*, *39*(2), 144–155. https://doi.org/10.1108/09590551111109094
19. Geismar, H. N., Dawande, M., Murthi, B. P. S., & Sriskandarajah, C. (2015). Maximizing

Revenue Through Two-Dimensional Shelf-Space Allocation. *Production and Operations Management*, *24*(7), 1148–1163. https://doi.org/10.1111/poms.12316

20. Guthrie, B., & Parikh, P. J. (2020). The rack orientation and curvature problem for retailers. *IISE Transactions*, 1–17. https://doi.org/10.1080/24725854.2020.1725253
21. Hansen, J. M., Raut, S., & Swami, S. (2010). Retail Shelf Allocation: A Comparative Analysis of Heuristic and Meta-Heuristic Approaches. *Journal of Retailing*, *86*(1), 94–105. https://doi.org/10.1016/j.jretai.2010.01.004
22. Hansen, P., & Heinsbroek, H. (1979). Product selection and space allocation in supermarkets. *European Journal of Operational Research*, *3*(6), 474–484. https://doi.org/10.1016/0377-2217(79)90030-4
23. Hariga, M. A., Al-Ahmari, A., & Mohamed, A.-R. A. (2007). A joint optimisation model for inventory replenishment, product assortment, shelf space and display area allocation decisions. *European Journal of Operational Research*, *181*(1), 239–251. https://doi.org/10.1016/j.ejor.2006.06.025
24. Heragu, S. S., & Kusiak, A. (1991). Efficient models for the facility layout problem. *European Journal of Operational Research*, *53*(1), 1–13. https://doi.org/10.1016/0377-2217(91)90088-D
25. Hübner, A. H., & Kuhn, H. (2012). Retail category management: State-of-the-art review of quantitative research and software applications in assortment and shelf space management. *Omega*, *40*(2), 199–209. https://doi.org/10.1016/j.omega.2011.05.008
26. Hübner, A., & Schaal, K. (2017). A shelf-space optimization model when demand is stochastic and space-elastic. *Omega*, *68*, 139–154. https://doi.org/10.1016/j.omega.2016.07.001
27. Hübner, A., Schäfer, F., & Schaal, K. N. (2020). Maximizing Profit via Assortment and Shelf-Space Optimization for Two-Dimensional Shelves. *Production and Operations Management*, *29*(3), 547–570. https://doi.org/10.1111/poms.13111

28. Hwang, H., Choi, B., & Lee, G. (2009). A genetic algorithm approach to an integrated problem of shelf space design and item allocation. *Computers & Industrial Engineering*, *56*(3), 809–820. https://doi.org/10.1016/j.cie.2008.09.012

29. Hwang, H., Choi, B., & Lee, M.-J. (2005). A model for shelf space allocation and inventory control considering location and inventory level effects on demand. *International Journal of Production Economics*, *97*(2), 185–195. https://doi.org/10.1016/j.ijpe.2004.07.003

30. Irion, J, Lu, J.-C., Al-Khayyal, F. A., & Tsao, Y.-C. (2011). A hierarchical decomposition approach to retail shelf space management and assortment decisions. *Journal of the Operational Research Society*, *62*(10), 1861–1870. https://doi.org/10.1057/jors.2010.147

31. Irion, Jens, Lu, J.-C., Al-Khayyal, F., & Tsao, Y.-C. (2012). A piecewise linearization framework for retail shelf space management models. *European Journal of Operational Research*, *222*(1), 122–136. https://doi.org/10.1016/j.ejor.2012.04.021

32. James V. Miranda, L. (2018). PySwarms: a research toolkit for Particle Swarm Optimization in Python. *The Journal of Open Source Software*, *3*(21), 433. https://doi.org/10.21105/joss.00433

33. Kennedy, J., & Eberhart, R. (1995). Particle swarm optimization. *Proceedings of ICNN'95 - International Conference on Neural Networks*, *4*, 1942–1948. https://doi.org/10.1109/ICNN.1995.488968

34. Kök, A. G., & Fisher, M. L. (2007). Demand Estimation and Assortment Optimization Under Substitution: Methodology and Application. *Operations Research*, *55*(6), 1001–1021. https://doi.org/10.1287/opre.1070.0409

35. Lim, A., Rodrigues, B., & Zhang, X. (2004). Metaheuristics with Local Search Techniques for Retail Shelf-Space Optimization. *Management Science*, *50*(1), 117–131. https://doi.org/10.1287/mnsc.1030.0165

36. Martello, S., & Toth, P. (1990). *Knapsack Problems*. John Wiley & Sons Ltd.

37. Montreuil, B. (1991). *A Modelling Framework for Integrating Layout Design and flow*

Network Design (pp. 95–115). https://doi.org/10.1007/978-3-642-84356-3_8

38. Mowrey, C. H., Parikh, P. J., & Gue, K. R. (2018). A model to optimize rack layout in a retail store. *European Journal of Operational Research*, *271*(3), 1100–1112. https://doi.org/10.1016/j.ejor.2018.05.062
39. Murray, C. C., Talukdar, D., & Gosavi, A. (2010). Joint Optimization of Product Price, Display Orientation and Shelf-Space Allocation in Retail Category Management. *Journal of Retailing*, *86*(2), 125–136. https://doi.org/10.1016/j.jretai.2010.02.008
40. Ozcan, T., & Esnaf, S. (2011). A heuristic approach based on artificial bee colony algorithm for retail shelf space optimization. *2011 IEEE Congress of Evolutionary Computation (CEC)*, 95–101. https://doi.org/10.1109/CEC.2011.5949604
41. Ozcan, T., & Esnaf, Ş. (2016). *Swarm Intelligence Approaches to Shelf Space Allocation Problem with Linear Profit Function* (pp. 22–41). https://doi.org/10.4018/978-1-5225-0075-9.ch002
42. Russell, R. A., & Urban, T. L. (2010). The location and allocation of products and product families on retail shelves. *Annals of Operations Research*, *179*(1), 131–147. https://doi.org/10.1007/s10479-008-0450-y
43. Shi, Y., & Eberhart, R. (1998). A modified particle swarm optimizer. *1998 IEEE International Conference on Evolutionary Computation Proceedings. IEEE World Congress on Computational Intelligence (Cat. No.98TH8360)*, 69–73. https://doi.org/10.1109/ICEC.1998.699146
44. Smith, S. A., & Agrawal, N. (2000). Management of Multi-Item Retail Inventory Systems with Demand Substitution. *Operations Research*, *48*(1), 50–64. https://doi.org/10.1287/opre.48.1.50.12443
45. Theodoridis, S. T., & Koutroumbas, K. (2009). *Pattern Recognition* (4th ed.). Elsevier.
46. Urban, T. L. (1998). An inventory-theoretic approach to product assortment and shelf-space allocation. *Journal of Retailing*, *74*(1), 15–35. https://doi.org/10.1016/S0022-

4359(99)80086-4

47. Urban, T. L. (2002). The interdependence of inventory management and retail shelf management. *International Journal of Physical Distribution & Logistics Management*, *32*(1), 41–58. https://doi.org/10.1108/09600030210415298

48. van Nierop, E., Fok, D., & Franses, P. H. (2008). Interaction Between Shelf Layout and Marketing Effectiveness and Its Impact on Optimizing Shelf Arrangements. *Marketing Science*, *27*(6), 1065–1082. https://doi.org/10.1287/mksc.1080.0365

49. Wirth, M. (2004). *Shape Analysis & Measurement Shape Analysis & Measurement*. Image Processing. http://www.cyto.purdue.edu/cdroms/micro2/content/education/wirth10.pdf

50. Yang, M.-H. (2001). An efficient algorithm to allocate shelf space. *European Journal of Operational Research*, *131*(1), 107–118. https://doi.org/10.1016/S0377-2217(99)00448-8

51. Yang, M.-H., & Chen, W.-C. (1999). A study on shelf space allocation and management. *International Journal of Production Economics*, *60–61*, 309–317. https://doi.org/10.1016/S0925-5273(98)00134-0

52. Zufryden, F. S. (1986). A Dynamic Programming Approach for Product Selection and Supermarket Shelf-Space Allocation. *Journal of the Operational Research Society*, *37*(4), 413–422. https://doi.org/10.1057/jors.1986.69

APPENDICES

Appendix A. Comparison of CPLEX and CP performances for subproblem (ii)

For the decomposition-based solution approach described in chapter-4, we tested both the CPLEX and CP algorithms for the reduced model. Recall that subproblem (ii) would need to be solved many times, one for each particle in each iteration. To be able to select between the two solvers, we created 11 cases and compared the solution times and quality (see Table A.1). In the table, Case Details column, Case, # of family, # of SKU, PW, and PH represent case number, number of families, planogram length, and planogram height, respectively. Under the CPLEX column, Time, Best Bound, Obj., and Gap represent solution time, best bound, best integer solution, and the gap between the best bound and integer solution, respectively. Under the CP column, Time, and Obj, represent the solution time and the objective function value. Clearly, the performance of CP was far more superior than CPLEX in solving the subproblem (ii).

Table A.1. CPLEX and CP performance comparison in solving subproblem (ii)

Case Details					CPLEX				CP	
Case	# of Family	# of SKU	PW	PH	Time (sec)	Best Bound	Obj	Gap	Time (Sec)	Obj
1	1	30	60	72	>9000	-	-	-	119	1399
2	1	30	30	72	>9000	1130	1071	6%	70	966
3	2	9	30	72	>1800	820	676	21%	10	650
4	1	45	30	72	>1800	429	-	-	119	405
5	2	24	30	72	>1800	429.8	392	9.25%	83	413
6	0	34	30	72	>1800	636	-	-	160	484
7	1	4	24	24	>1800	332	120	175%	0.5	120
8	1	4	48	48	>1800	603	483	25.00%	1.5	483
9	2	26	30	72	>1800	828	751	10%	35	766
10	2	26	60	72	>1800	1998	-	-	120	1590
11	4	3	15	15	381	71	71	0%	0.3	71

In table A.1 Case Details column, Case, # of family, # of SKU, PW, and PH represent case number, number of families, planogram length, and planogram height respectively. In the CPLEX column, Time, Best Bound, Obj., and Gap represent solution time, best bound, best integer solution, and the gap between the best bound and integer solution respectively. In CP column Time, and Obj, represent the solution time and the objective function value.

Appendix B. PSO-CP Convergence Table

We tested the convergence of the PSO-CP algorithm in 3 cases. We solved each case 3 times using 6 particles and recorded global best solutions and particle best solutions and represent them in Table B.1.

Table B.1. PSO -CP Convergence

Case Name	**Runs**	**Objective Value of Particles**						**Global Best**	**MAPE Between**	
		P-1	**P-2**	**P-3**	**P-4**	**P-5**	**P-6**		**Particles**	**Runs**
N5F2W24H60	1	97.27	97.27	97.27	97.27	97.27	97.27	97.27	0 %	0 %
	2	97.27	97.27	97.27	97.27	97.27	97.27	97.27	0 %	0 %
	3	97.27	97.27	97.27	97.27	97.27	97.27	97.27	0 %	0 %
N10F2W36H72	1	221.92	221.92	221.92	221.92	222.59	221.92	222.59	0.25 %	0 %
	2	221.92	221.92	221.92	221.92	221.92	221.92	221.92	0 %	0.3%
	3	221.92	221.92	222.59	222.59	222.59	221.92	222.59	0.15 %	0 %
N10F3W36H72	1	255.4	255.4	255.4	255.4	255.4	255.4	255.4	0 %	0 %
	2	255.4	255.4	255.4	255.4	255.4	255.4	255.4	0 %	0 %
	3	255.4	255.4	255.4	255.4	255.4	255.4	255.4	0 %	0 %
								Average	0.04%	0.03

In Table B.1 MAPE represents the Mean Absolute Percentage Error between particles and between runs. Table B.1 shows that the average MAPE between particles was 0.04% and the average MAPE between global best objective function values was 0.03%.

Appendix C. Experiment Results

Table C.1 shows the details of the test-runs completed for shape variation and space fitness experiments.

Table C.1. Experiment Results
(Note: For each case, the first row indicates revenue in $ and the second row indicates run time in seconds.)

	SF = 0.28 (PW:60, PH:60)					**SF = 0.23 (PW:72, PH:60)**					**SF = 0.20 (PW:84, PH:60)**					**SF = 0.16 (PW:106, PH:60)**				
Case	Min Shelf Length					Min Shelf Length					Min Shelf Length					Min Shelf Length				
	12”	24”	36”	48”	60”	12”	24”	36”	48”	60”	12”	24”	36”	48”	60”	12”	24”	36”	48”	60”
HM-A	3351	3351	3351	3351	3351	4191	4191	4191	4191	4191	4779	4779	4779	4779	4779	5871	5871	5871	5871	5871
	1187	782	743	623	893	1236	977	882	1015	1099	1262	912	859	805	1016	1103	1118	960	876	860
HM-B	3351	3340	3276	3276	3276	3950	3938	3928	3928	3928	4632	4576	4576	4576	4576	5778	5778	5764	5764	5764
	864	607	30	26	15	735	233	16	26	34	748	119	17	15	26	1007	518	32	37	21
HM-C	3560	3560	3560	3560	3560	3740	3740	3740	3740	3740	4760	4760	4760	4760	4760	5960	5960	5960	5960	5960
	747	698	598	609	787	688	617	418	458	588	668	794	621	685	970	720	653	503	526	536
HM-D	3600	3600	3600	3600	3600	3600	3600	3600	3600	3600	4500	4500	4500	4500	4500	6180	6180	6180	6180	6180
	698	691	539	504	1113	1514	969	1087	728	723	987	943	921	815	1289	1252	1066	1124	1005	1675
LHM-A	3600	3600	3300	3300	3300	4150	4100	4100	3850	3850	4750	4700	4650	4650	4650	6150	6150	6150	6150	6150
	1176	1191	109	153	36	560	228	491	93	23	612	297	171	209	583	836	154	60	14	20
LHM-B	3287	3277	3203	3203	3203	4011	3900	3807	3780	3780	4680	4644	4608	4375	4375	6034	5950	5875	5861	5785
	398	134	354	15	9	1088	177	21	22	15	185	88	7	12	13	91	32	28	181	15
LHM-C	3297	3297	3270	3270	3270	4092	3855	3855	3855	3855	4526	4490	4454	4346	4346	4950	4950	4950	4950	4860
	1357	78	14	23	100	438	387	49	114	113	214	63	76	17	15	526	297	35	232	33
LHM-D	3376	3245	3173	3173	3173	4104	4098	4092	3989	3989	4403	4403	4385	4339	4339	5812	5471	5486	5486	5369
	1711	363	35	45	85	705	820	315	107	110	65	191	87	124	426	1797	1374	61	93	66
HT-A	3457	3449	2238	2238	2238	4161	4127	4089	2960	2960	4913	4823	4757	3610	3610	6255	6133	6164	6122	4826
	1271	737	119	68	116	1687	2235	738	69	59	1829	1383	1146	56	36	1946	1833	1347	1489	66
HT-B	3468	3365	3094	3094	3094	4124	4011	3987	3647	3647	4811	4762	4630	4337	4337	6070	5984	5859	5859	5801
	1278	1357	879	705	740	1412	1198	2200	887	1134	1754	1685	1797	1099	1882	1789	1782	1645	2844	1738
HT-C	3481	3367	3083	3083	3083	4219	4166	3910	3767	3767	4759	4719	4615	4471	4471	6031	6039	5907	5901	5507
	2219	1747	682	641	1557	1751	1872	1972	744	774	1677	2407	1553	831	1312	2053	3089	1621	2728	1699
HT-D	3369	3345	3083	3083	3083	4135	4052	3910	3767	3767	4890	4783	4753	4471	4471	6134	6059	5992	5500	5301
	1373	2063	667	686	753	1734	1731	2475	1077	633	2690	1878	2439	1096	1927	1811	3119	2272	1779	1736

Appendix D. Case Study Results

In Table D.1, columns W, H represents the width and height of each SKU. The family and price of each SKU are given in Family and P columns. Org. face column represents the number of faces in the original planogram. Columns Lower and Upper show the lower and upper bounds for the number of faces. The number of faces created by the improved design is represented in Imp. face column. We also represent the area of each SKU in the Area column.

Table D.1 shows that the highest increase in the number of faces is in family 1. Note that in family 1, SKU sizes are smaller compared to other families. PSO-CP was able to utilize the previously unused space by increasing the facings of smaller products and grouping them on a separate shelf. We also observe that even though the SKU prices are lower in family 1, the PSO-CP model still preferred to allocate more from family 1. It seems like SKU dimensions have more impact on revenue than SKU prices for this planogram. These observations show that a greedy SKU allocation can result in a sub-optimal design.

Table D.1. Case study data and results

UPC	W	H	Family	P ($)	Org. face	Lower	Upper	Imp. face	Area
1	2	3	1	15.99	1	1	2	2	6
2	5	7	3	24.99	1	1	2	1	35
3	5	8	4	29.99	1	1	2	1	40
4	3	4	1	10.99	1	1	2	2	12
5	5	7	4	19.99	1	1	2	1	35
6	2	2	2	39.99	1	1	2	1	4
7	6	3	1	1.99	2	1	3	3	18
8	3	5	2	3.99	1	1	2	1	15
9	3	5	1	14.99	1	1	2	2	15
10	2	3	2	25.92	1	1	2	2	6
11	4	6	4	29.99	1	1	2	1	24
12	4	4	3	2.99	1	1	2	2	16
13	3	5	2	11.99	1	1	2	1	15
14	5	7	4	29.99	1	1	2	1	35
15	3	4	1	1.99	1	1	2	1	12
16	2	5	1	13.99	1	1	2	2	10
17	3	2	2	34.99	1	1	2	1	6
18	3	5	2	3.99	1	1	2	1	15
19	5	7	4	19.99	1	1	2	1	35
20	4	6	2	19.99	1	1	2	1	24
21	2	2	2	34.99	1	1	2	1	4
22	4	2	3	1.99	1	1	2	2	8
23	3	4	2	1	1	1	2	1	12
24	4	6	3	34.99	1	1	2	1	24
25	5	7	4	34.99	1	1	2	1	35
26	4	6	3	34.63	1	1	2	1	24
27	4	6	4	29.99	1	1	2	2	24
28	3	4	1	1.99	1	1	2	1	12
29	4	6	3	30.99	1	1	2	1	24
30	3	5	2	7.99	1	1	2	1	15
31	2	3	1	15.99	1	1	2	2	6
32	3	3	1	11.99	1	1	2	2	9
33	3	4	2	1	1	1	2	1	12
34	3	3	1	7.99	1	1	2	2	9
35	3	4	2	1	1	1	2	1	12
36	4	8	3	3.99	1	1	2	1	32
37	5	7	3	19.99	1	1	2	1	35
38	3	3	1	43.5	1	1	2	2	9
39	5	7	4	9.49	1	1	2	1	35
40	3	4	1	1.99	1	1	2	1	12
41	6	3	1	1.99	2	1	3	2	18
42	3	4	1	11.99	1	1	2	2	12
43	5	7	4	19.99	1	1	2	1	35
44	2	4	1	11.99	1	1	2	2	8
45	3	5	2	3.99	1	1	2	1	15
46	5	7	3	19.99	1	1	2	1	35
47	3	4	1	1.07	1	1	2	1	12
48	3	5	2	8.7	1	1	2	1	15
49	4	6	2	9.99	1	1	2	1	24
50	4	6	3	21.09	1	1	2	1	24
51	3	5	2	3.99	1	1	2	1	15
52	2	2	2	19.99	1	1	2	1	4
53	2	2	2	21.99	1	1	2	2	4
54	6	7	4	27.99	1	1	2	1	42
55	5	7	3	19.99	1	1	2	1	35